SUPPORTING INFORMATION

Non-polymeric Nanogels as Versatile Nanocarriers. Intracellular Transport of the Photosensitizers Rose Bengal and Hypericin for Photodynamic Therapy

Ana Torres-Martínez,[a] Begoña Bedrina,[a] Eva Falomir,[a] María J. Marín,[b] César A. Angulo-Pachón,[a] Francisco Galindo[a,*] and Juan F. Miravet[a,*]

[a]Departament de Química Inorgànica i Orgànica, Universitat Jaume I, Avda. Sos Baynat s/n, 12071 Castelló de la Plana, Spain. E-mail: francisco.galindo@uji.es , miravet@uji.es

[b]School of Chemistry, University of East Anglia, Norwich Research Park, Norwich NR4 7TJ, UK

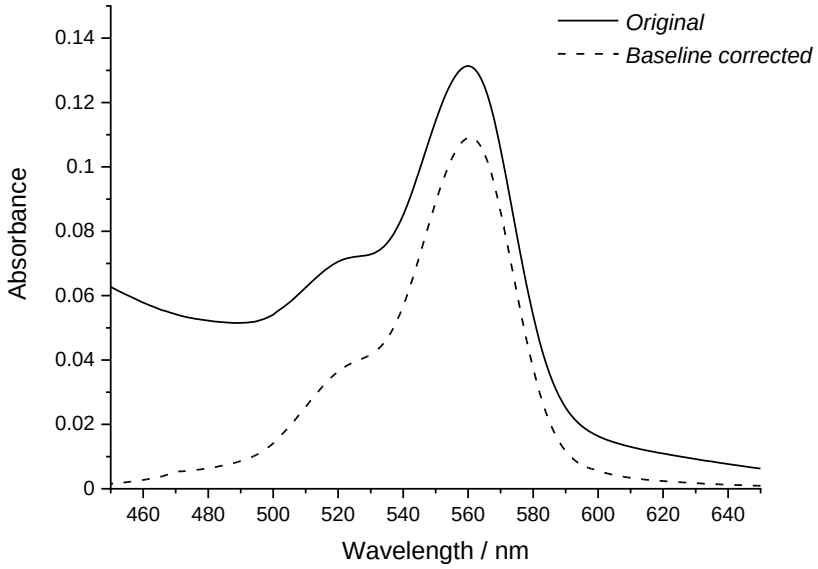

Figure S1. Original and baseline corrected UV-Vis absorption spectrum of a sample of RB@**1** in PBS.

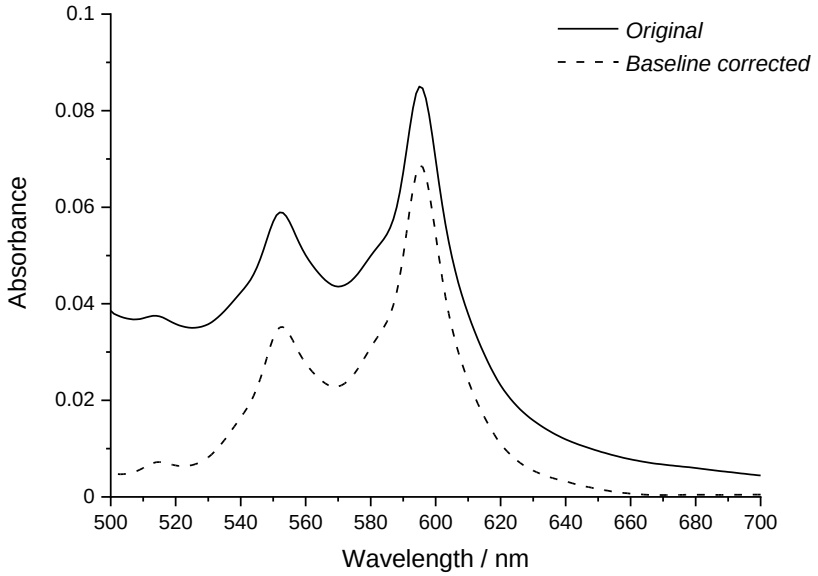

Figure S2. Original and baseline corrected UV-Vis absorption spectrum of a sample of HYP@**1** in PBS.

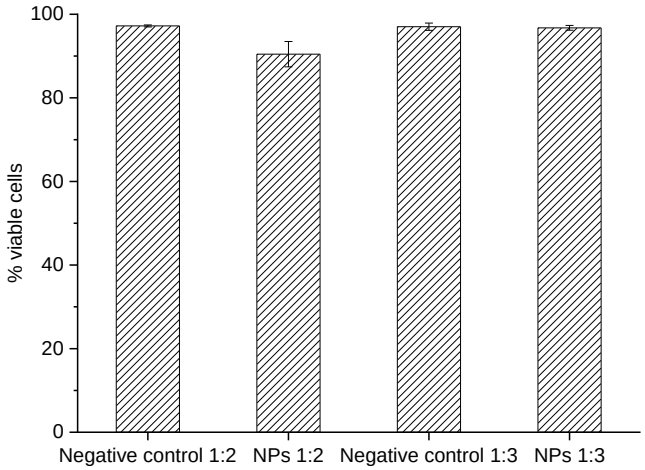

Figure S3. Trypan blue cell viability assays on HT-29 cells incubated with nanogel samples of **1** (NPs in the graph) diluted 1:2 and 1:3.

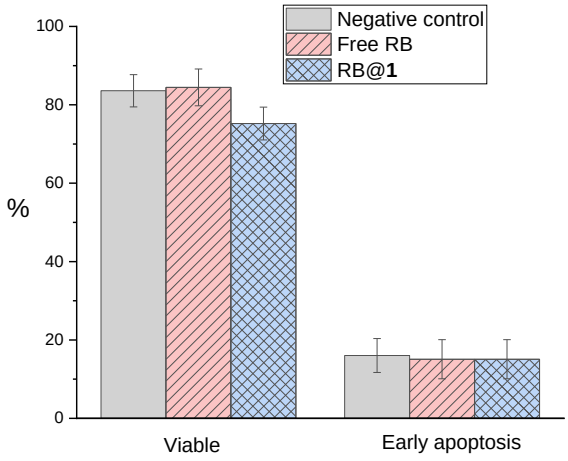

Figure S4. Cell viability and early apoptosis obtained for non-irradiated control experiments with HT-29 cells loaded with RB as a photosensitizer, using annexin V-FITC/propidium iodide staining. Negative control corresponds to cells incubated with PBS. The results are the average of three different batches analyzed in duplicate (average [RB] in culture media was 2 μM).

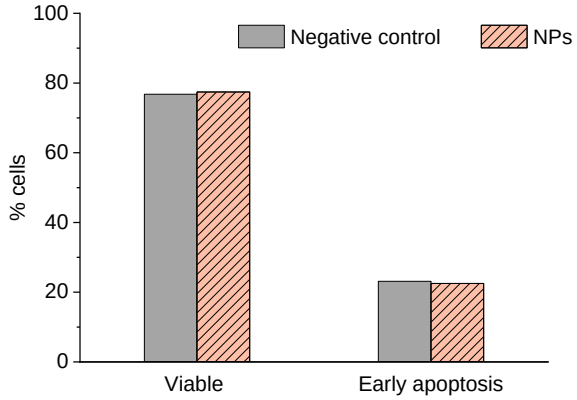

Figure S5. Cell viability and early apoptosis obtained for PDT experiments (2 min irradiation) of HT-29 cells incubated with unloaded nanogels samples, using Annexin V-FITC/propidium iodide staining. Negative control corresponds to cells incubated with PBS.

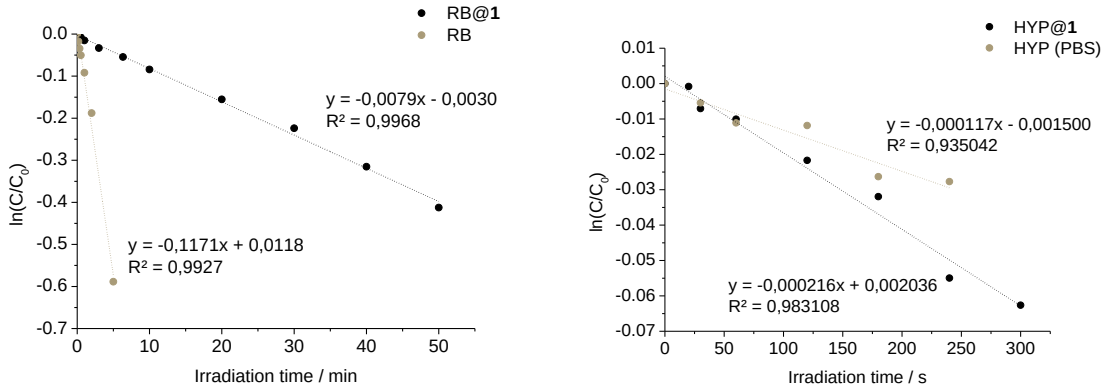

Figure S6. Representative examples of the linear fit of ABDA fluorescence emission (λ_{ex} 380 nm, λ_{em} 407 nm) decay as a function of the irradiation time in the presence of PS@**1** and PS in PBS (left: RB@**1** and RB, right: HYP@**1** and HYP).

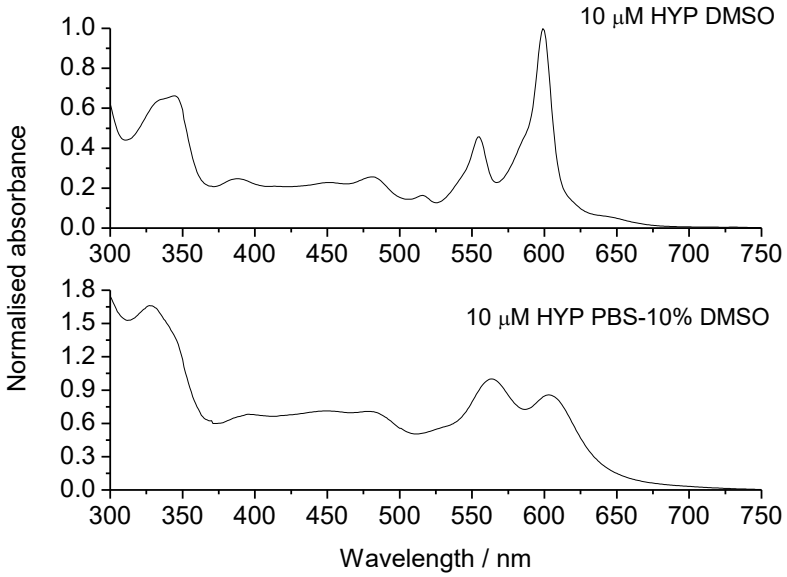

Figure S7. Normalised UV-Vis absorption spectra of a 10 μM hypericin solution in DMSO (top) and in PBS, 10% DMSO (bottom).

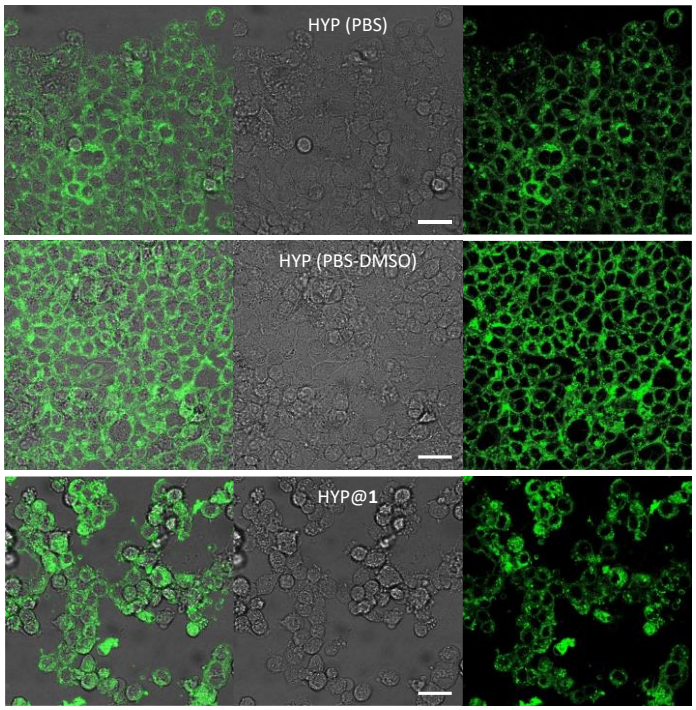

Figure S8. Images from confocal laser scanning microscopy; λ_{ex} 561 nm. The fluorescence intensity has been enhanced to show the localization of the dye. From left to right: merged, DIC and green channels. Scale bar = 27 μm.

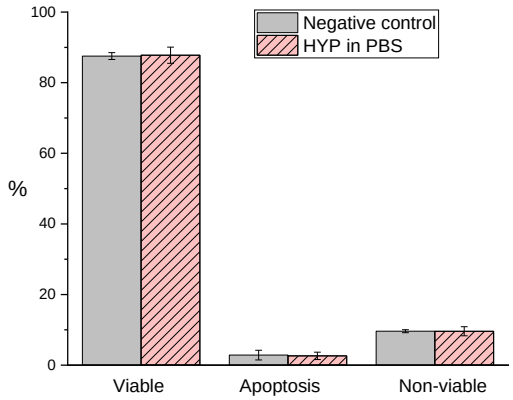

Figure S9. Cell viability and apoptosis obtained for PDT experiments (2 min irradiation) with HT-29 cells and HYP as a photosensitizer (HYP in PBS), using YO-PRO®-1/propidium iodide staining. Negative control corresponds to cells incubated with PBS. The results are the average of three different batches analyzed in duplicate (average [HYP] in culture media was 0.02 μM).

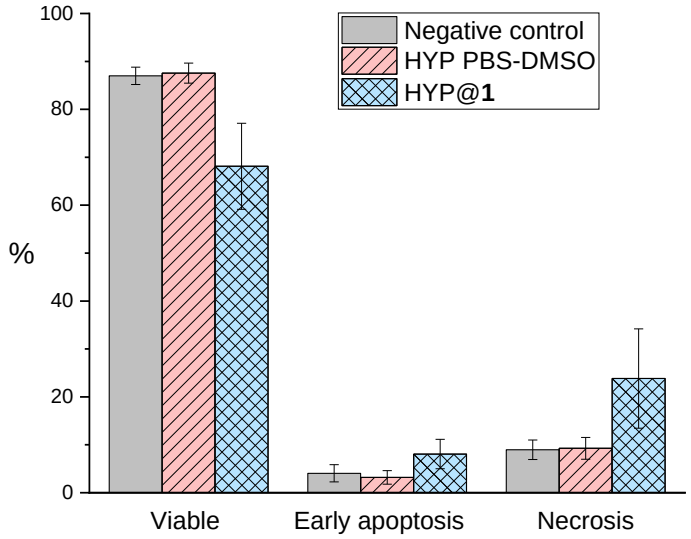

Figure S10. Results obtained by flow cytometry of cell viability and apoptosis in PDT experiments without irradiation with HT-29 cells and HYP as a photosensitizer. YO-PRO®-1/propidium iodide was used for staining. Negative control corresponds to cells incubated with PBS. The results are the average of three different batches analyzed in duplicate. [HYP] = 0.2 μM.

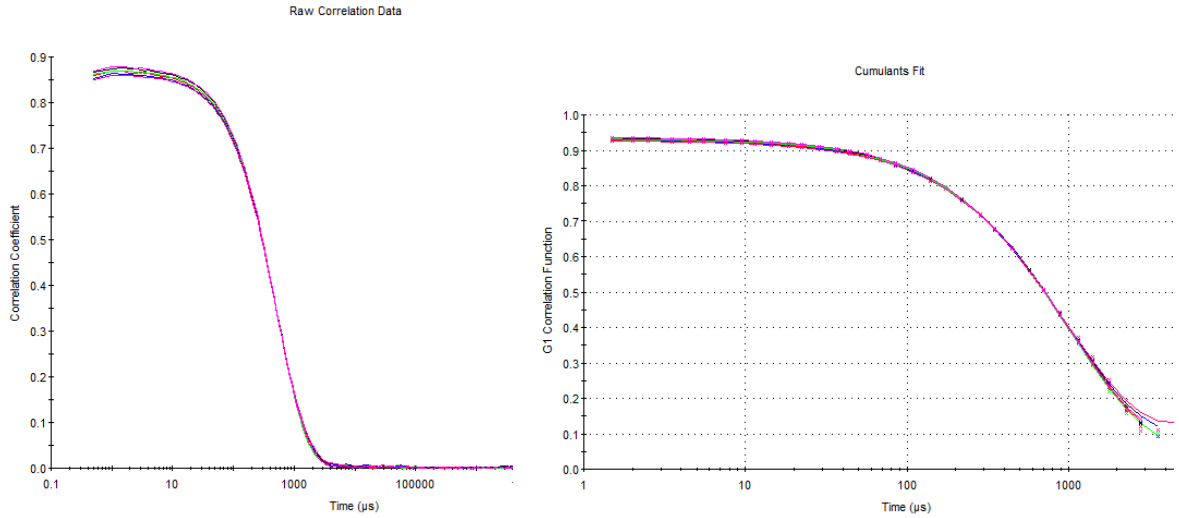

Figure S11. Superposition of raw correlation data and cumulants fit from 6 measurements (11 scans each) by DLS of a sample of RB@**1**

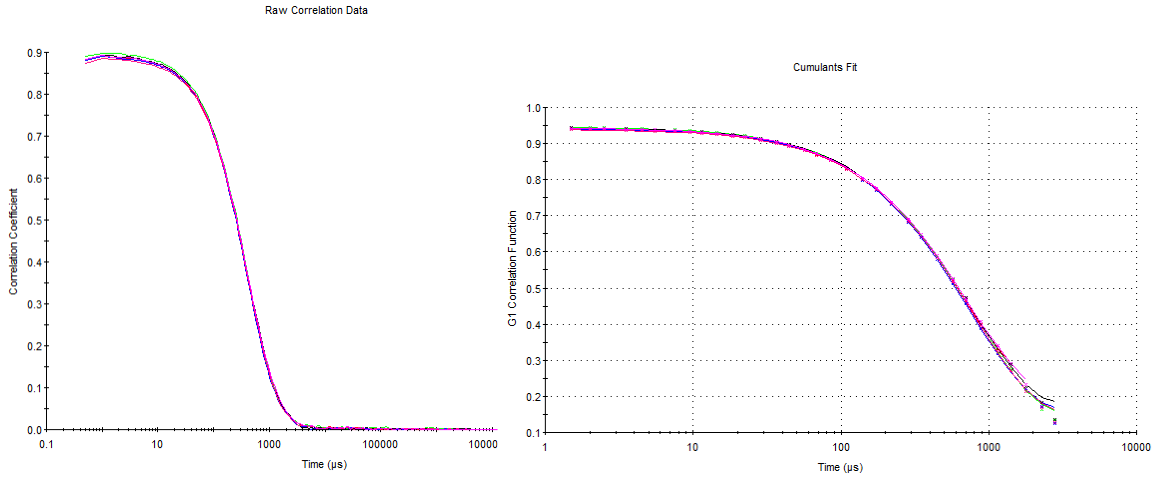

Figure S12. Superposition of raw correlation data and cumulants fit from 6 measurements (11 scans each) by DLS of a sample of HYP@**1**.

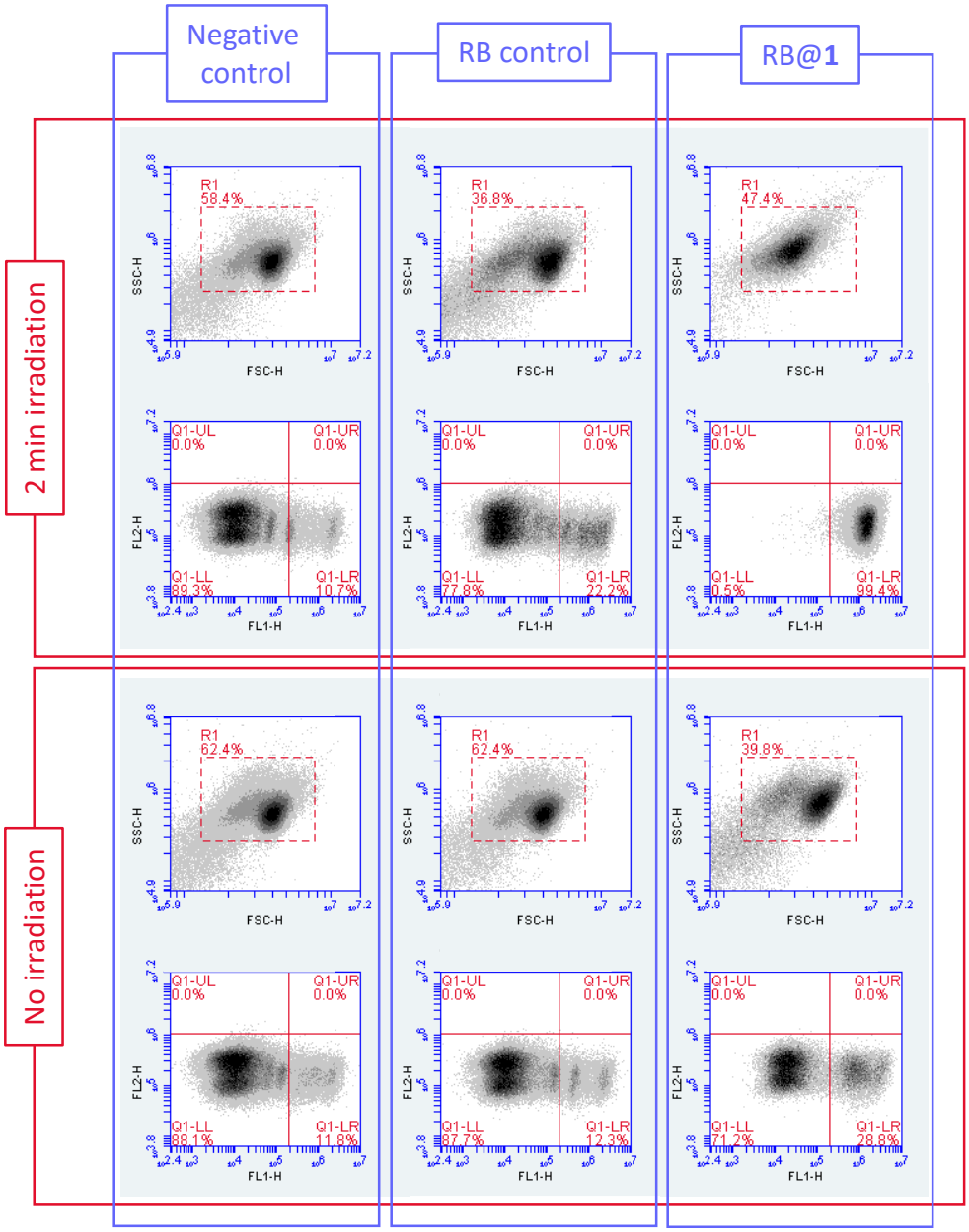

Figure S13. Representative dot plot obtained by flow cytometry in the analysis of HT-29 cells incubated with RB@**1**.

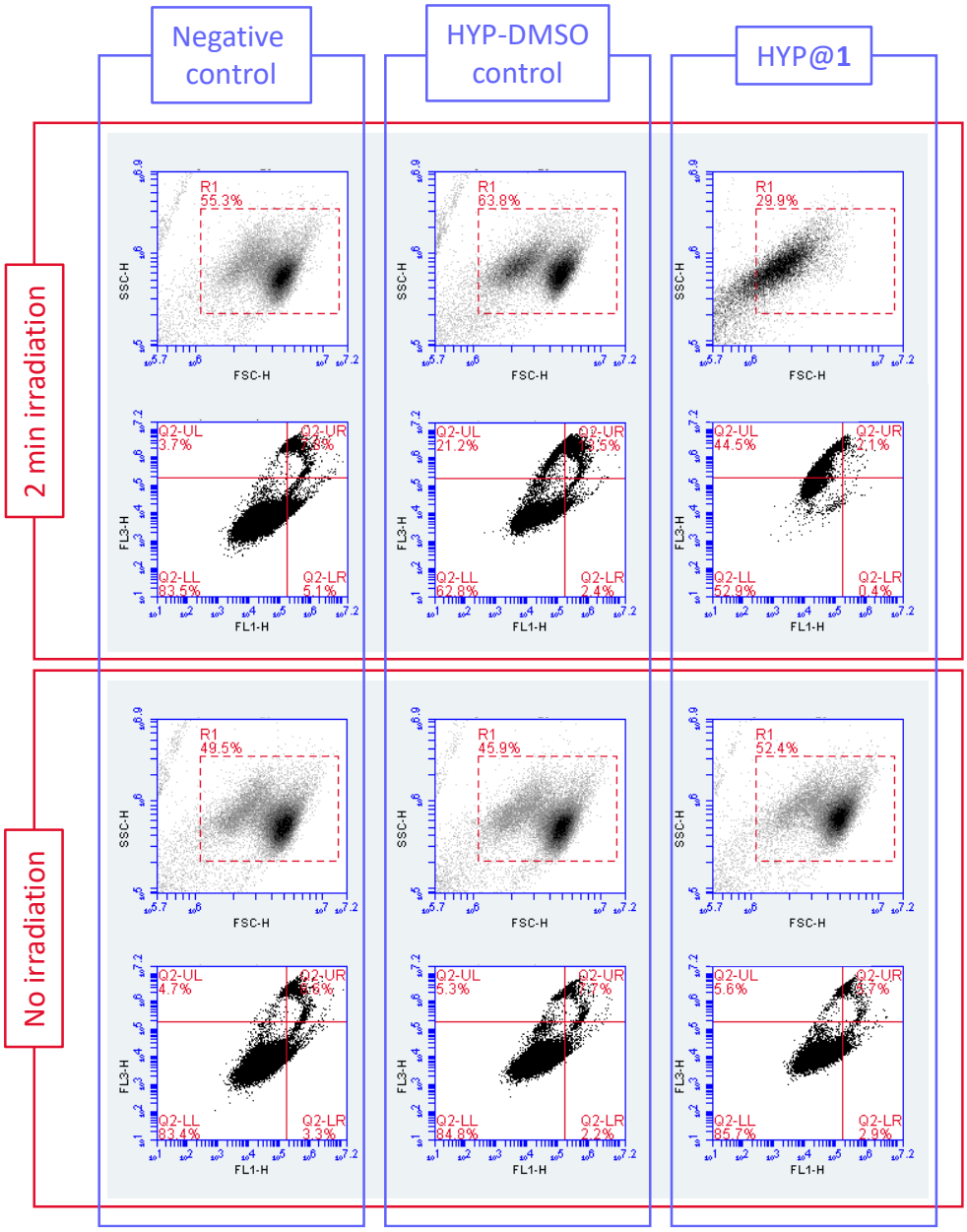

Figure S14. Representative dot plot obtained by flow cytometry in the analysis of HT-29 cells incubated with HYP@**1**.

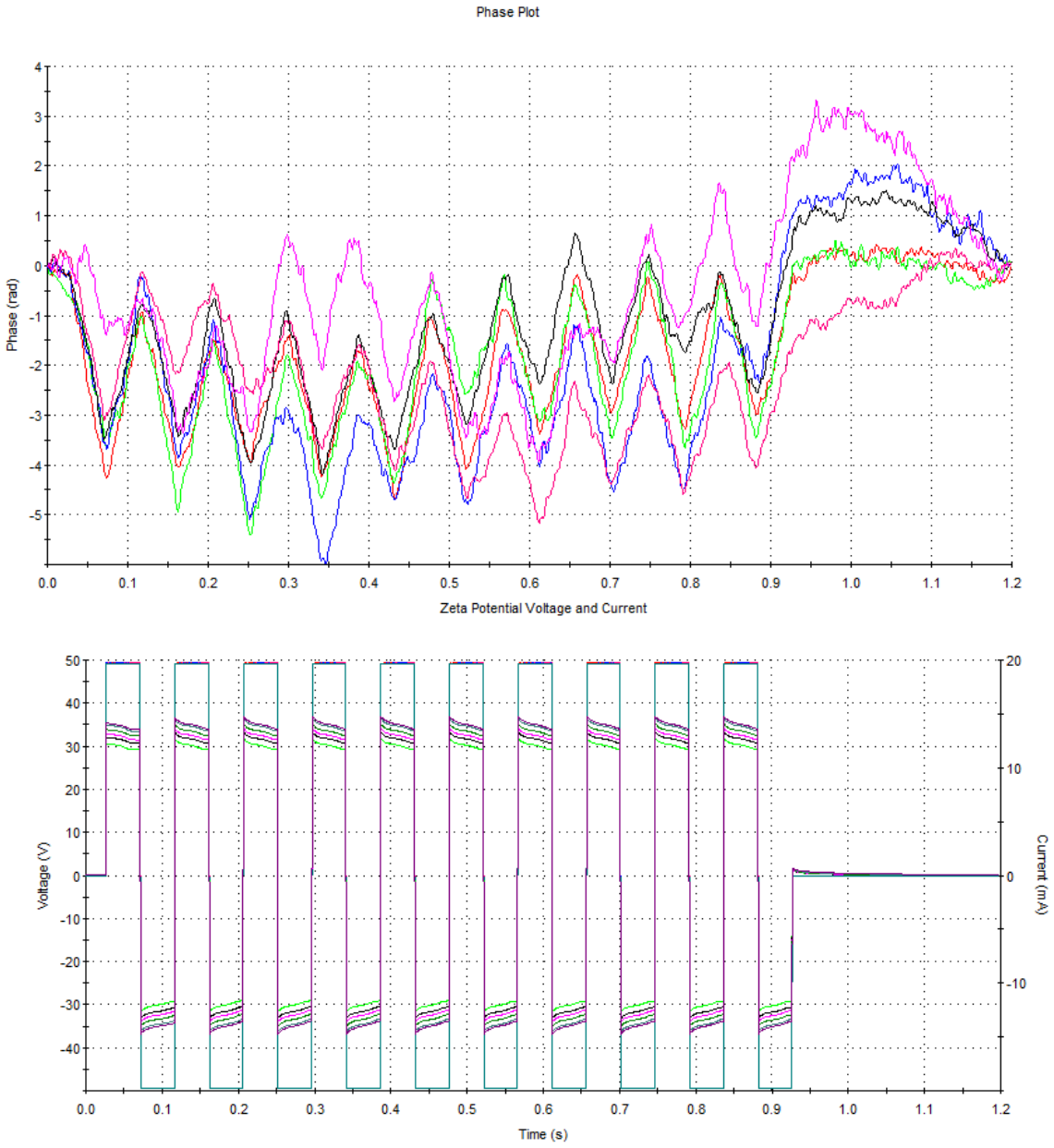

Figure S15. Phase plot (top) and voltage and current plot (bottom) obtained in the determination of the Z-potential of RB@**1** nanogels.

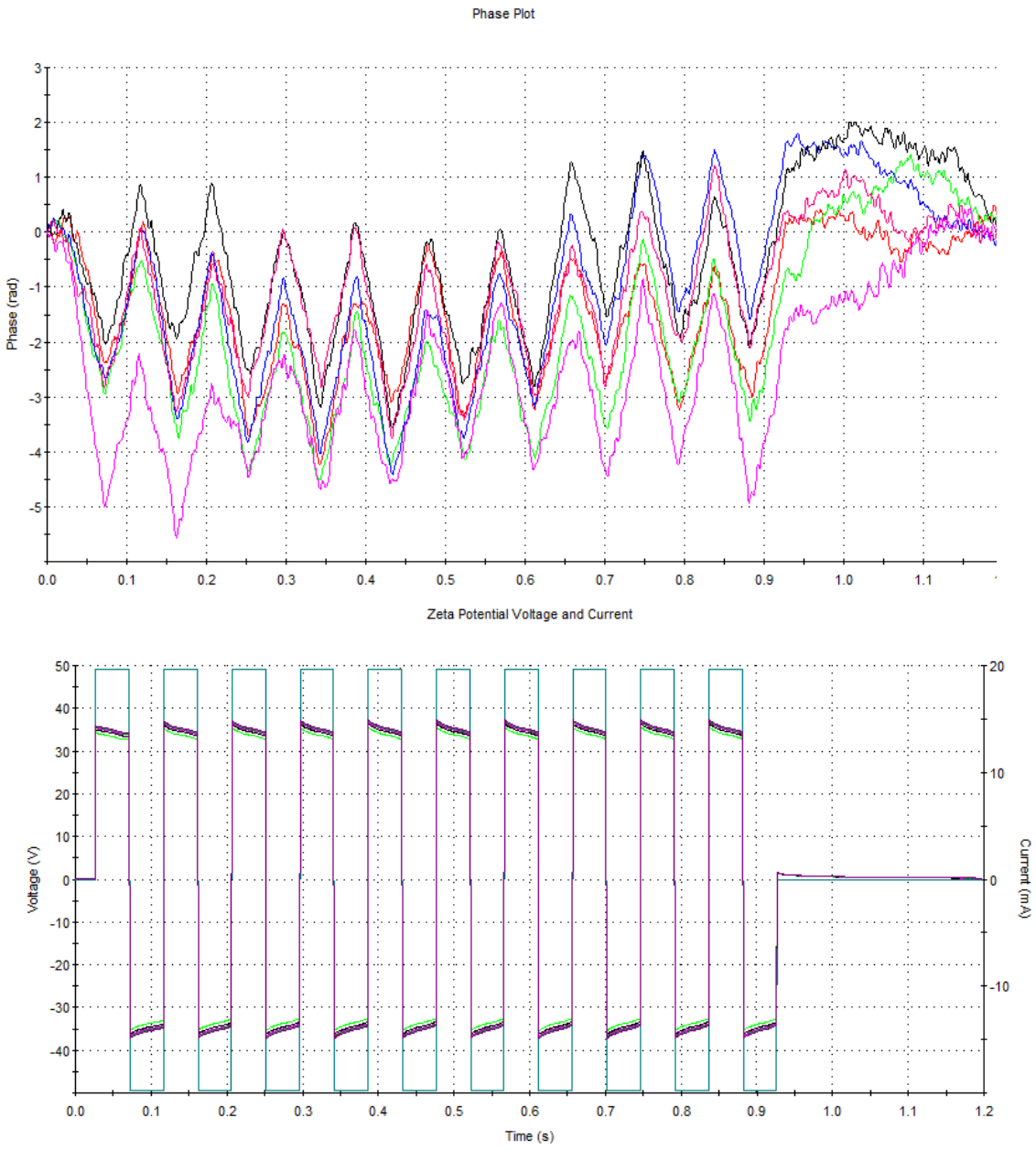

Figure S16. Phase plot (top) and voltage and current plot (bottom) obtained in the determination of the Z-potential of HYP@**1** nanogels.